# Effect of the feedback loops on the frequency response in the tryptophan operon of *Bacillus subtilis*

Alberto Nakauma, and Jesús Rodríguez-González
Centro de Investigación y de Estudios Avanzados del IPN, Unidad Monterrey, Vía del Conocimiento 201, Parque de Investigación e Innovación Tecnológica, 66600 Apodaca NL, México
anakauma@cinvestav.mx, jrodriguez@cinvestav.mx

***Abstract*—Bacteria must respond in an appropriate way to external stimuli to overcome the challenges of the environment. In this paper we introduce a linear mathematical model for the tryptophan operon pathway in *Bacillus subtilis*. This model considers the transport of tryptophan from extracellular to intracellular level. We applied frequency analysis to determine the response of the *trp* operon to changes in extracellular tryptophan. We studied the effect that has the two negative feedback loops on the frequency response in the *trp* operon. We found that wild-type bacterium and mutants without any of the two feedback loops have a behavior corresponding to a low-pass filter. Besides, our results suggest that both feedback loops help *B. subtilis* to respond in an appropriate way due to without any of them, the response time is longer than the duplication time of the bacterium which could affect its adaptation to environment.**

***Keywords- frequency response; cut-off frequency; feedback loop; synthesized tryptophan, external tryptophan.***

## I. INTRODUCTION

Bacteria are always exposed to external conditions that are very changeable in which must respond in an appropriate way to survive. There is a plethora of ways to study the bacterial response to changeable external stimuli. The frequency response characterization is an experimental or theoretical method to probe this behavior in genetic systems [1].

There are some mathematical models and experimental works based on the frequency response of microorganisms. For instance, the frequency response in bacterial chemotaxis is studied in [2,3]. The response of S*accharomyces cerevisiae* to periodic changes in carbon source is studied in [4]. In [5,6] is studied the response of the osmotic regulation to dynamic stimuli in *S. cerevisiae* too, and the frequency response on the tryptophan operon of *Escherichia coli* is studied in [7]. In a graph of frequency response, we can point out the cut-off frequency that is related with the response time of the system, i.e. the time it takes to transmit the signal from receptors to target molecules [5]. If the cut-off frequency is at high frequency, then, the response time is fast, otherwise it is slow.

*Bacillus subtilis* is a Gram-positive soil bacterium. Two negative feedback loops, in their molecular mechanism, regulate the biosynthesis of tryptophan aminoacid via the *trp* operon [8]. The activity of the *trp* operon can be affected due to *B. subtilis* can obtain this aminoacid for uptake from extracellular medium. Having in mind the discussion in the previous paragraphs, the objective of this work was to investigate how changes the frequency response in the *trp* operon in wild-type bacterium versus strains without negative feedback loops and strains with strong feedback loops. To do this we made use of linear control theory tools [9,10].

## II. METHODS

### A. Molecular description of the trp operon

The *trp* operon in *B. subtilis* controls the production of tryptophan inside the cell. It utilizes two negative feedback loops: transcription attenuation and enzyme inhibition. When the tryptophan is plentiful the operon is repressed. There are other key molecular processes including transcription, translation and synthesis of tryptophan and AT protein (Fig. 1). Tryptophan is feed-backed to inhibit anthranilate synthase enzyme if tryptophan level is high, two tryptophan molecules bind to anthranilate synthase (the first enzyme in the biosynthesis pathway) reducing the rate of biosynthesis of tryptophan, this is the enzyme inhibition negative feedback loop. Transcription attenuation is controlled by TRAP and AT proteins. When tryptophan is plentiful, TRAP is activated with eleven molecules of tryptophan and the nascent mRNA wraps the activated TRAP halting the transcription process. In conditions of tryptophan starvation, *at* operon is active and AT protein is produced. AT protein binds to activated TRAP protein inactivating it. The *at* operon is regulated by sensing

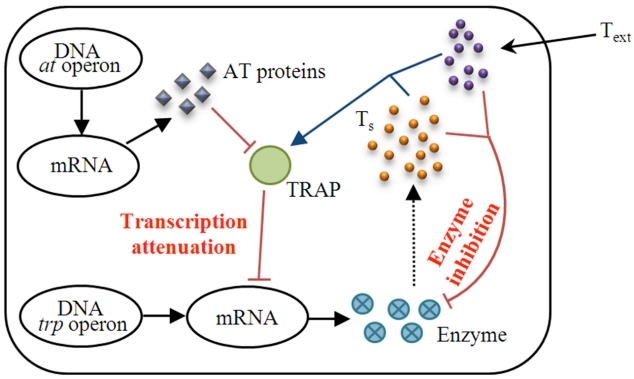


Figure 1. Network scheme of the *trp* operon. The total tryptophan, $T_T$, is formed by synthesized tryptophan, $T_S$, produced by biosynthetic pathway (dashed line) and instantaneous extracellular tryptophan, $T_{ext}$, uptake from the medium. Intracellular tryptophan inhibits enzyme activity and actives TRAP. Activated TRAP attenuates transcription of enzymes necessary for the synthesis of tryptophan ($T_S$). AT protein produced by *at* operon inhibits activated TRAP.

uncharged $tRNA^{Trp}$. When uncharged $tRNA^{Trp}$ concentration is high, there is not enough intracellular tryptophan, the *at* operon is activated producing AT protein, then, activated TRAP proteins are inhibited [11]. The reader interested in the full explication of molecular mechanism may consult [8] and [11].

### *B. Mathematical model for tryptophan production*

In this section the *trp* operon model developed by [12] is modified to consider $T_{ext}$ following [13]. The dynamics of mRNA ($M$), anthranilate synthase ($E$), synthesized tryptophan ($T_S$) and AT protein ($A$) concentrations are governed by the following non-linear ordinary differential equations:

$$\dot{M} = k_M D P_A(T_T, A) - (\lambda_M + \mu)M, \tag{1}$$

$$\dot{E} = \frac{1}{2} k_p M - (\lambda_E + \mu)E, \tag{2}$$

$$\dot{T}_S = k_N E \Psi(T_T) - \rho \frac{T_S}{K_\rho + T_S} - \mu T_S, \tag{3}$$

$$\dot{A} = \beta \Omega(T_T)\Theta(T_T) - \mu A, \tag{4}$$

$$T_T = T_S + T_{ext}. \tag{5}$$

We consider that $T_{ext}$ is uptaken into the cell instantly. Then, the total internal tryptophan, $T_T$, is the algebraic sum of synthesized tryptophan ($T_S$) and external tryptophan ($T_{ext}$). Parameter $k_M$ is the transcription rate, $k_p$ is the translation rate, $k_N$ is the tryptophan synthesis rate and $\beta$ is the protein AT synthesis rate. $D$ is the concentration of *trp* promoter. Parameters $\lambda_M$ and $\lambda_E$ are the degradation rate of mRNA and enzyme, respectively. The concentration of biomolecules could decrease due to the bacterial growth, μ. Factor ½ in (2) is because two polypeptides are required to form the enzyme. Term $\rho T_S/(K_\rho+T_S)$ is the tryptophan consumption due to the protein synthesis, where $\rho$ is the maximum tryptophan consumption rate, $K_\rho$ is the saturation constant of tryptophan consumption. To complete the model, the following definitions are required:

$$P_A(T_T, A) = \frac{K_D}{K_D + \left(\frac{T}{K_T + T}\right)^{11} \left(\frac{K_A}{K_A + A}\right)^4 Y_T}, \tag{6}$$

$$\Psi(T) = \left(\frac{K_Q}{K_Q + T_T}\right), \tag{7}$$

$$\Omega(T) = \frac{K}{K + T_T}, \tag{8}$$

$$\Theta(T) = \frac{1 + 3\frac{\alpha T_T}{K_G + T_T} + 3\left(\frac{\alpha T_T}{K_G + T_T}\right)^2}{\left(1 + \frac{\alpha T_T}{K_G + T_T}\right)^3}. \tag{9}$$

Where the regulation mechanisms in the *at* operon are given by functions $\Omega(T_T)$ and $\Theta(T_T)$. The functions $P_A(T_T,A)$ and $\Psi(T_T)$ represent transcription attenuation and enzyme inhibition mechanism in the *trp* operon, respectively. $K_D$ is the dissociation constant between activated TRAP protein and leader region of the *trp* operon. $K_T$ represents the dissociation constant between one molecule of tryptophan and one empty site in TRAP protein, $K_A$ is the dissociation constant between AT protein and one site in activated TRAP protein, $K_Q$ is the dissociation constant between one molecule of tryptophan and its binding site in antranilato synthase. Parameter $K$ equals $G_{Tot}K_G/K_Z$, where $G_{Tot}$ is the total concentration of $tRNA^{Trp}$, $K_G$ is the dissociation constant of the complex formed by uncharged $tRNA^{Trp}$ and one molecule of tryptophan, $K_Z$ is the dissociation constant of complex formed by leader region of the *at* operon and one molecule of uncharged $tRNA^{Trp}$. Parameter α is the rate between $G_{Tot}$ and the dissociation constant of the *trp* codon and charged $tRNA^{Trp}$.

The values of all parameters used are referred from work [12] (see Table 1).

### *C. Linearization of the trp operon mathematical model*

To obtain the frequency response of the *trp* operon system, first the non-linear equations were linearized as follow:

$$\dot{x} = \begin{pmatrix} \dot{M} & \dot{E} & \dot{T}_S & \dot{A} \end{pmatrix}^T = \mathrm{A}x + \mathrm{B}u, \tag{10}$$

where $x$ is the vector of variables $M$, $E$, $T_S$ and $A$, $u$ is the input vector, $T_{ext}$. A is the state matrix, also known as Jacobian matrix, and B is the input matrix, both are evaluated at steady-state ($M^*$, $E^*$, $T_S^*$, $A^*$). The steady-state is reached when $\dot{M} = 0$, $\dot{E} = 0$, $\dot{T}_S = 0$ and $\dot{A} = 0$, with a nominal value of $T_{ext}$ ($T_{ext}^*$). A and B are given by:

$$\mathrm{A} = \begin{pmatrix} \frac{\partial \dot{M}}{\partial M} & \frac{\partial \dot{M}}{\partial E} & \frac{\partial \dot{M}}{\partial T_S} & \frac{\partial \dot{M}}{\partial A} \\ \frac{\partial \dot{E}}{\partial M} & \frac{\partial \dot{E}}{\partial E} & \frac{\partial \dot{E}}{\partial T_S} & \frac{\partial \dot{E}}{\partial A} \\ \frac{\partial \dot{T}_S}{\partial M} & \frac{\partial \dot{T}_S}{\partial E} & \frac{\partial \dot{T}_S}{\partial T_S} & \frac{\partial \dot{T}_S}{\partial A} \\ \frac{\partial \dot{A}}{\partial M} & \frac{\partial \dot{A}}{\partial E} & \frac{\partial \dot{A}}{\partial T_S} & \frac{\partial \dot{A}}{\partial A} \end{pmatrix}_{M^*,E^*,T_S^*,A^*,T_{ext}^*}, \tag{11}$$

$$\mathrm{B} = \begin{pmatrix} \frac{\partial \dot{M}}{\partial T_{ext}} \\ \frac{\partial \dot{E}}{\partial T_{ext}} \\ \frac{\partial \dot{T}_S}{\partial T_{ext}} \\ \frac{\partial \dot{A}}{\partial T_{ext}} \end{pmatrix}_{M^*,E^*,T_S^*,A^*,T_{ext}^*}. \tag{12}$$

TABLE I. PARAMETERS OF THE *TRP* MODEL [12]

| Parameter | Value | Parameter | Value |
|---|---|---|---|
| $k_M$ | 16 $min^{-1}$ | $K_\rho$ | 10 μM |
| $k_P$ | 20 $min^{-1}$ | $K_D$ | 1.2x$10^{-4}$ μM |
| $k_N$ | 7.3x$10^{4}$ $min^{-1}$ | $K_T$ | 0.4 μM |
| $\beta$ | 6x$10^{-4}$ μM$min^{-1}$ | $K_A$ | 0.6 μM |
| $D$ | 3.3x$10^{-4}$ μM | $Y_T$ | 8x$10^{-2}$ μM |
| $\lambda_M$ | 0.53 $min^{-1}$ | $K_Q$ | 4.1 μM |
| $\lambda_E$ | 0.0 $min^{-1}$ | $K$ | 2x$10^{17}$ μM |
| $\mu$ | 6x$10^{-3}$ $min^{-1}$ | $K_G$ | 1.6 μM |
| $\rho$ | 24.3 μM$min^{1}$ | α | 95 |

The next step was to apply the Laplace transform to (10) and obtain the transfer function:

$$H(s) = \frac{T_S(s)}{T_{ext}(s)}, \tag{13}$$

where $T_S(s)$ and $T_{ext}(s)$ are the Laplace transform of $T_S$ (output variable) and $T_{ext}$ (input variable). The transfer function, $H(s)$, is a complex ratio of polynomials, where $s=i\omega$. The gain and phase were evaluated as:

$$G_{dB}(\omega) = 20\log_{10}|H(s)|, \tag{14}$$

$$\angle G(\omega) = \arg H(s). \tag{15}$$

Finally, the gain $G_{dB}(\omega)$ and the phase $\angle G(\omega)$ are shown in a Bode plot to obtain the frequency response.

We obtained the frequency response for the wild-type system for different $T_{ext}$ concentrations. We carried out several simulations to get the range of linear response. (plots not shown).The maximum of tryptophan that *B. subtilis* could synthesize $T_{S\_max}$, is reached when $T_{ext}$=0 μM. We obtain a linear response when the output variable $T_S$ between 10-90% of the maximum concentration, $T_{S\_max}$.

The frequency response for different strains was carried out for $T_{ext}$=0.3$T_{S_max}$. These $T_{ext}$ concentrations were used because ensure the region of linearity in the system. So, for each strain there is a steady-state, depending on the concentration of $T_{ext}$.

## III. RESULTS

We numerically solved the set of non-linear equations (1-4) and the linearized model (10) with the fourth-order Runge-Kutta method implemented in MATLAB (The MathWorks, Natick, MA).

### *A. Dynamic of the synthesis of tryptophan*

To analyze the regulatory behavior of the *trp* operon in wild-type strain, we numerically solved the set of non-linear equations (1-4) and carried out simulations with the following set of initial conditions: M(0)=0 μM, E(0)=0 μM, $T_S$(0)=0 μM

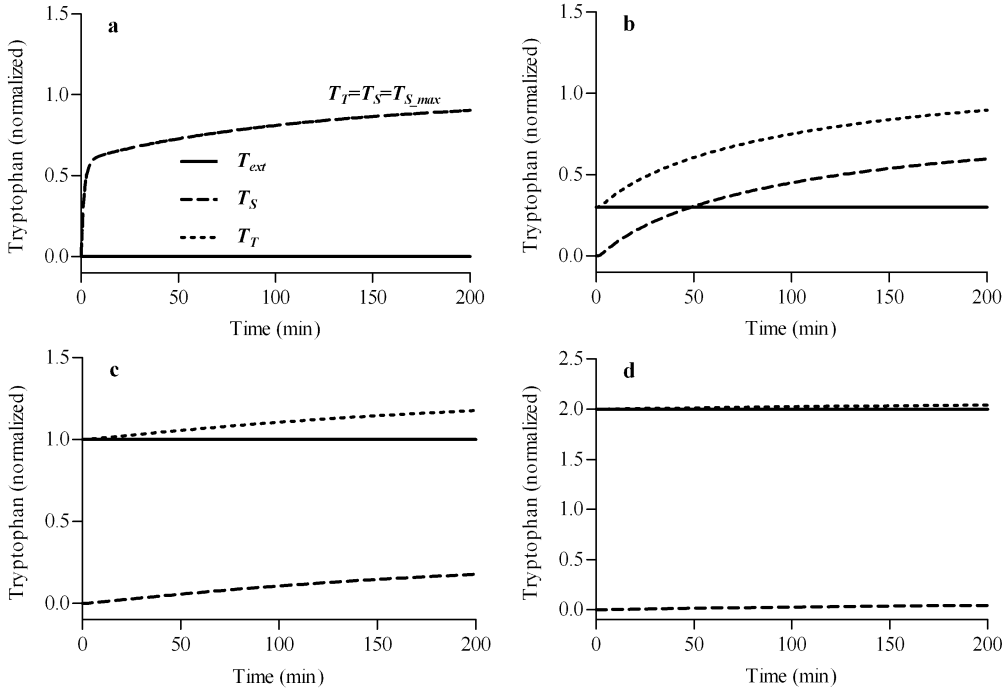


Figure 2. Dynamic simulation of the *trp* operon of a wild type strain for different amount of $T_{ext}$. a) In absence of $T_{ext}$ all total tryptophan is due to $T_S$, this is the maximum amount of $T_S$ that the strain could synthesize ($T_{S\_max}$). When there is external tryptophan in the medium, $T_S$ decreases with b) $T_{ext}$=0.3$T_{S_max}$ and c) $T_{ext}$=1.0$T_{S_max}$. d) But, when $T_{ext}$>2$T_{S_max}$, the *trp* operon is repressed, so $T_S$≈0. Tryptophan concentration was normalized by 38 μM.

and A(0)=0 μM for different values of $T_{ext}$.

Fig. 2 shows the dynamic behavior of intracellular tryptophan concentration at various $T_{ext}$ concentrations: $0.0T_{S\_max}$, $0.3T_{S\_max}$ , $0.7T_{S\_max}$ , and $2.0T_{S\_max}$. As can be observed in Fig. 2a, when $T_{ext}$ =0 μM, the maximum amount of intracellular tryptophan is synthetized. With an increase in $T_{ext}$ concentration, $T_T$ results from contributions by both, synthetized and transported tryptophan, see (5) and Fig. 2b and 2c. A twofold increase in $T_{ext}$ concentration leads to complete repression of the *trp* operon, then $T_S \approx 0$, Fig. 2d.

To test the linear model feasibility, we linearized the wild-type system considering $T_{ext}= 0.3T_{S\_max}$ and impulse response between non-linear (1-4) and linear system (10) were simulated. Fig. 3 shows the impulse response between both models with different values of perturbation on $T_S$. We can see that our linearized model reproduces the non-linear behavior. This makes us confident to attempt further analyze.

### *B. Frequency response of wild-type and feedback-less mutants*

Our next task was to explore the frequency response in the wild-type strain using different values of $T_{ext}$ from $0.1T_{S\_max}<T_{ext}<0.9T_{S\_max}$. We can see the Bode plot in Fig. 4. Our simulations show that the gain Bode plot is a low-pass filter, Fig. 4a. Furthermore, as we have seen, a similar cut-off frequency and slope are obtained with $T_{ext}$ in the interval: $0.1T_{S\_max}<T_{ext}<0.9T_{S\_max}$. But the gain is reduced if $T_{ext}$ increases. The corresponding phase Bode plot is shown in Fig. 4b. We can see a similar phase response for different values of $T_{ext}$. The phase shift varies from π/2 to π due to the response is in anti-phase with the stimulus, i.e. if there is $T_{ext}$ in the medium, then $T_S$ decreases and vice versa.

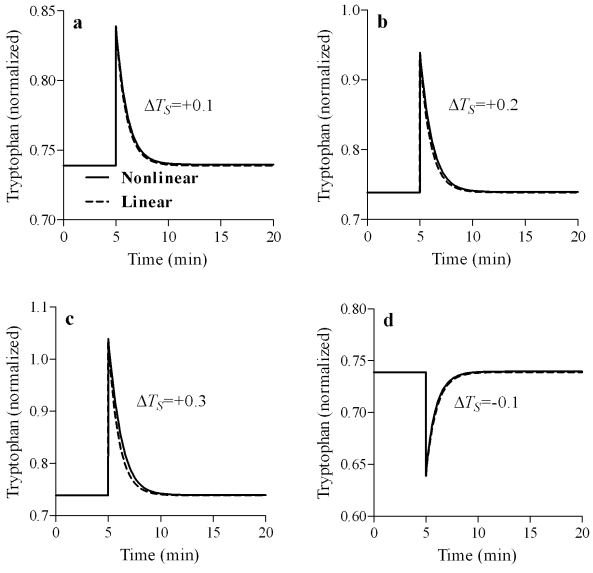


Figure 3. Impulse response of the linear and non-linear models. The linear model is valid for small perturbations on $T_S$, in a), b), c) and d) the linear and non-linear models match very well. Linearization was carried out with $T_{ext}=0.3T_{S\_max}$. Tryptophan concentration was normalized by 38 μM.

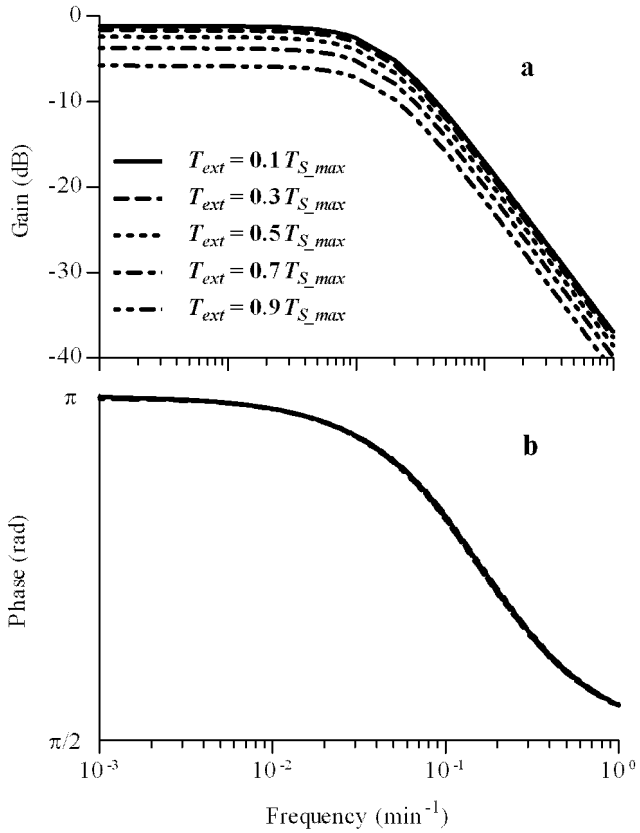


Figure 4. Bode plot of wild type strain. a) When $T_{ext}$ is high the maximum gain decreases. However, the cut-off frequencies are the same in all cases. b) The phase is the same and shifts between π/2 and π in all cases.

To analyze the influence of both feedback loops on the frequency response, we repeated the previous simulations with mutants of *B. subtilis* that lack enzyme inhibition or transcription attenuation mechanism.

We can represent a strain without transcription attenuation feedback loop setting $P_A(T_T,A)=1$ and $T_{ext}=0.3T_{S\_max}$. Fig. 5 shows the Bode plot for this strain. We can see a small difference in the cut-off frequency and similar slope compared with wild-type strain. The phase behavior is similar in both cases.

We represent a strain without enzyme inhibition feedback loop setting $\Psi(T_T)=1$, and $T_{ext}= 0.3T_{S\_max}$. Fig. 5 shows our simulation results. We can see that a bacterium without enzyme inhibition feedback loop has the maximum gain around -100 dB. The cut-off frequency value decreases notably while the slope increases. The phase shift varies from π to -π/2.

### *C. Frequency response of mutants with stronger feedback loops*

Recall that the *trp* operon in *B. subtilis* comprises two different regulatory mechanisms, both operating through negative feedback loops. Our next task was to investigate the effect of making stronger each feedback loop in the *trp* operon.

To test the influence of transcription attenuation feedback loop when is made stronger, we decreased the value of

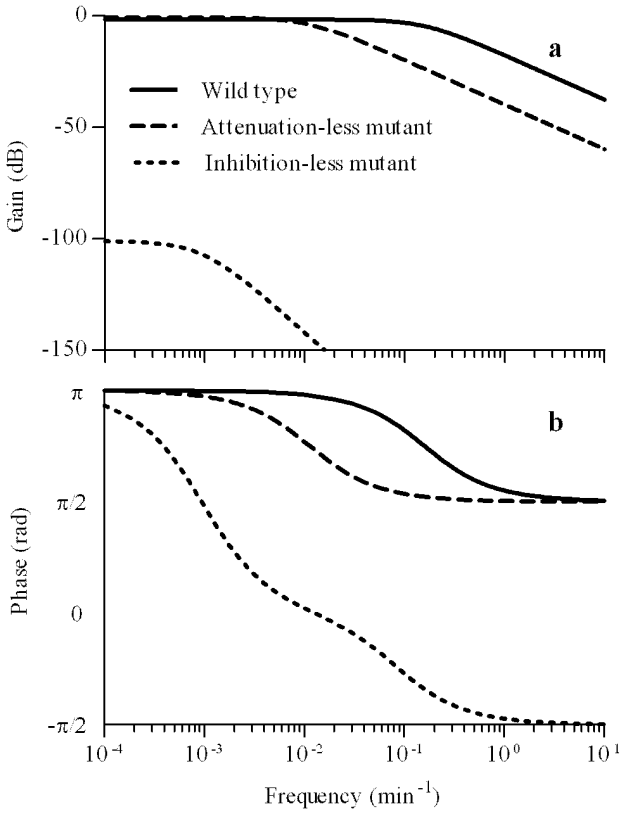


Figure 5. Frequency response of strains without feedback loops. Comparison in the a) gain and b) phase of wild type with different strains. The mutant that lacks the transcriptional mechanism has the cut-off frequency fewer and the phase shift faster than wild type. The gain of the mutant without the attenuation mechanism is small and the cut-off is shifted at low frequencies, the phase change from positive to negative side.

parameter $K_D$ up to $10^{-5}$ times in order to obtain the frequency response whit this mutant. In Fig. 6 we can see that when transcription attenuation is made stronger ($K_D$ is reduced) its cut-off frequency is right shifted. But, the gain is reduced. To corroborate our results, we carried out a simulation of a bacterium that lacks this feedback loop ($K_D$ is increased). The gain Bode plot is in agreement with above experiment, Fig. 5.

Finally, to test the influence of enzyme inhibition feedback loop when is made stronger, we decreased the value of parameter $K_Q$ up to $10^{-5}$ times. In Fig. 7 we can see that when enzyme inhibition is made stronger ($K_Q$ is reduced) its cut-off frequency is right shifted. Again, to corroborate our results, we carried out a simulation of a bacterium that lacks this feedback loop ($K_Q$ is increased). The gain Bode plot is in agreement with above experiment, Fig. 5.

## IV. Discussion and Conclusion

In this work, a linear mathematical model of the *trp* operon of *B. subtilis* was developed. Our model was based on a non-linear model developed in [12]. We modified the model to take into account the transport of $T_{ext}$ to intracellular level according to [13]. The regulatory effect of the *trp* operon was verified in wild-type bacterium. When $T_{ext}$=0 μM, the model reproduces results from [12]. Besides, the regulatory effect is consistent with [13] when $T_{ext}$>0 μM.

The linearization is valid for small perturbations around steady-state, because the linear model matches with the dynamic of the non-linear model with small changes on $T_S$ concentration. Hence, our linear model is enough to carry out frequency domain analysis.

Our next task was to obtain the frequency response of the wild-type bacterium. We used the transfer function of the *trp* operon to calculate the Bode plot. We found that the gain is just affected when $T_{ext}$ is high due to the repression of the *trp* operon, i.e. when $T_{ext}$ is near or higher than concentration of $T_{S\_max}$, the synthesis of $T_S$ is few or near to zero and the system do not respond even if we put more $T_{ext}$. This behavior is logic since the bacterium will not produce more $T_S$ when $T_{ext}$ is plentiful. Besides, the slope is -20 dB per decade that is typical for first order low-pass filter [14]. Moreover, phase shift shown a regular behavior in all cases, changing just in the positive side, between π/2 and π. Changes in positive side are due to the fact that input $T_{ext}$ and output $T_S$ are in anti-phase, i.e. if we put $T_{ext}$, then $T_S$ concentration decreases, and otherwise if we remove $T_{ext}$. Besides, having a range of π/2

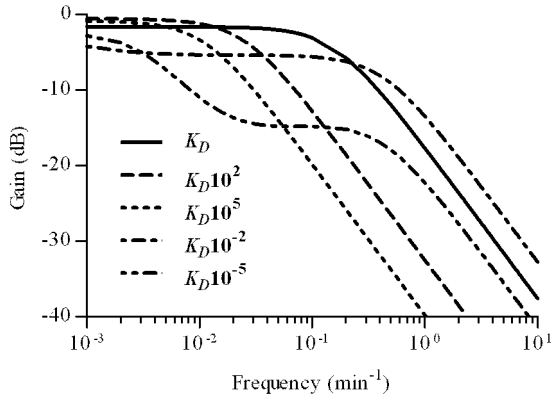


Figure 6. The gain Bode plot of a stronger attenuation feedback loop. $K_D$ was increased and decreased in two and five order of magnitude in order to weaken and strengthen the attenuation feedback loop, respectively. A stronger feedback changes the cut-off frequency to high frequencies, but the maximum gain is reduced. The weak feedback is to corroborate the experiment in Fig. 5 and has the same effect as a strain that lacks this feedback loop.

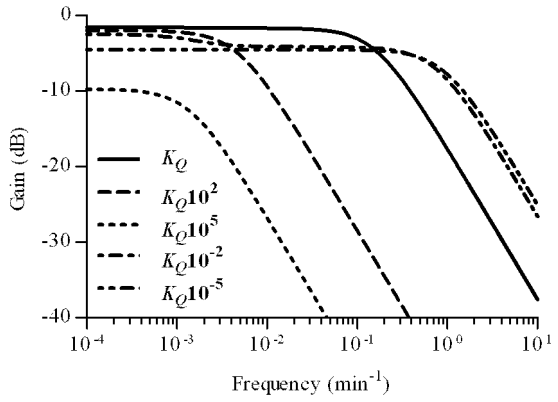


Figure 7. The gain Bode plot of a stronger inhibition feedback loop. We increased and decreased in two and five order of magnitude $K_Q$ in order to make weaker or stronger the feedback, respectively. The stronger feedback shifts the cut-off frequency to high frequencies, but the maximum gain is small compared with the wild-type strain. The weak feedback is to corroborate the experiment in Fig. 5 and has the same effect as a strain that lacks this feedback loop.

where the phase shift can change, allows *B. subtilis* response relatively fast in a wide range of frequencies. These results obtained on gain (slope) and phase (range that can change the phase) correspond to a behavior of a first order filter [15].

To investigate the influence of the feedback loops on the frequency response of the *trp* operon, we carried out simulations and compare the frequency responses of wild-type versus attenuation-less and inhibition-less mutants. In the attenuation-less mutant, the cut-off frequency is changed to low frequencies. Also the phase shift is higher than wild-type bacterium. Since that the cut-off frequency is related to the response time of a biological system [5], our results show that the response time of attenuation-less mutant is longer than wild-type system. The inhibition-less mutant shows the lowest cut-off frequency, this suggest that enzyme inhibition is the first mechanism that respond for homeostasis of *B. subtilis* due to inhibition-less mutant has the longest response time. In some sense is logic to think this because the biosynthesis pathway is a fast mechanism. The gain is also affected due to the maximum gain decreases near to -100 dB. The slope also changes to -40 dB per decade, and the phase change from positive to negative side. All these effects on the frequency response of the inhibition-less mutant indicate that inhibition mechanism has a key role in the fast response of *B. subtilis* to $T_{ext}$ changes.

We were also interested in the dynamic behavior of the *trp* operon when individual feedback loops are stronger. Two different sets of *in silico* experiments were performed in which the feedback strength of the attenuation and inhibition loops are varied. In each set, the loop subjected to change has its strength altered to both sides of its basal level, with the lower end of $10^{-5}$ times the basal value and the higher end of $10^{5}$ times the basal value. According to our results, a stronger attenuation loop results in a high cut-off frequency. Furthermore, a stronger inhibition loop results in a more flat frequency response and a high cut-off frequency. The gain is affected in both cases. In [7], the authors found that a stronger negative feedback loop shifts the cut-off frequency to high frequencies and the maximum gain is decreased. Our results are in agreement with [7].

The results of this study indicate that the wild-type and mutant systems behave as a low-pass filter. Our results are in agreement with [16] who show that, in terms of its signal processing capabilities, a feedback loop functions as a low-pass filter.

In conclusion, frequency response analysis provides knowledge about the response time of the *trp* operon of *B. subtilis* to any shape of stimulus. That it is true because in principle any temporal signal could be decompose into its sinusoidal components [9]. The results of this study indicate that *B. subtilis* have evolved its regulation mechanisms in the *trp* operon to response in an appropriate way to perturbations of $T_{ext}$. If there is not one of the regulation mechanisms, the bacterium shows a slow response. But, if the one of the regulation feedbacks is strong, the response is fast with a low gain. These changes in the strength of the feedback loops from the basal level could affect the adaptive capability of *B. subtilis* to respond to external tryptophan.

## ACKNOWLEDGMENT

This work was supported by CONACYT (Consejo Nacional de Ciencia y Tecnología) under grant: 105649.

## REFERENCES

[1] J. Ang, B. Ingalls, and D. McMillen, "Probing the input-output behavior of biochemical and genetic systems system identification methods from control theory," Meth. Enzymol., vol. 487, pp. 279-317, 2011.

[2] J. E. Segall, S. M. Block, and H. C. Berg, "Temporal comparisons in bacterial chemotaxis," Proc. Natl. Acad. Sci. U.S.A, vol. 83, pp 8987-8991, Dec. 1986.

[3] A. Hamadeh et al., "Feedback control architecture and the bacterial chemotaxis network", PLoS Comput. Biol., vol. 7, pp. e1001130, May 2011.

[4] M. R. Bennett et al., "Metabolic gene regulation in a dynamically changing environment," Nature, vol. 454, pp. 1119-1122, Aug. 2008.

[5] P. Hersen, M. N. McClean, L. Mahadevan, and S. Ramanathan, "Signal processing by the HOG MAP kinase pathway," Proc. Natl. Acad. Sci. U.S.A, vol. 105, pp. 7165-7170, May 2008.

[6] J. T. Mettetal, D. Muzzey, C. Gómez-Uribe, and A. van Oudenaarden, "The frequency dependence of osmo-adaptation in Saccharomyces cerevisiae," Science, vol. 319, pp. 482-484, Jan. 2008.

[7] B. P. Ingalls, "A Frequency Domain Approach to Sensitivity Analysis of Biochemical Networks," J. Phys. Chem. B, vol. 108, pp. 1143-1152, Jan. 2004.

[8] C. Yanofsky, "The different roles of tryptophan transfer RNA in regulating trp operon expression in E. coli versus B. subtilis," Trends Genet, vol. 20, pp. 367-374, Aug. 2004.

[9] E. W. Kamen and B. S. Heck, Fundamentals of Signals and Systems Using the Web and MATLAB®, 3rd ed., Prentice Hall, 2006.

[10] K. Ogata, Modern Control Engineering, 4rd ed., Prentice Hall, 2001.

[11] P. Gollnick, P. Babitzke, A. Antson, and C. Yanofsky, "Complexity in regulation of tryptophan biosynthesis in Bacillus subtilis," Annu. Rev. Genet., vol. 39, pp. 47-68, 2005.

[12] C. Zamora-Chimal and J. Rodríguez-González, "Influence of the feedback loops in the trp operon of B. subtilis on the system dynamic response and noise amplitude" unpublished.

[13] S. Bhartiya, S. Rawool, and K. V. Venkatesh, "Dynamic model of Escherichia coli tryptophan operon shows an optimal structural design," Eur. J. Biochem., vol. 270, pp. 2644-2651, Jun. 2003.

[14] J. D. Lenk, Simplified design of filter circuits. Newnes, 1999.

[15] L. J. Tung and B. W. Kwan, Circuit analysis. World Scientific, 2001.

[16] C. Rao, D. Wolf, and A. Arkin, "Control, exploitation and tolerance of intracellular noise.". Nature. Vol. 420, pp. 231-237, 2002.